Noorhana Yahya

ADVANCED STRUCTURED MATERIALS 5

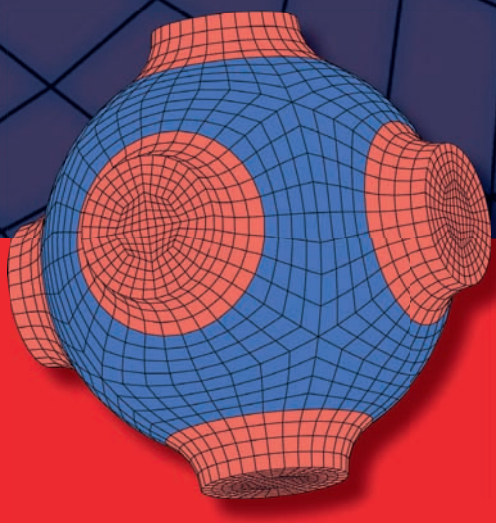

Carbon and Oxide Nanostructures

Synthesis, Characterisation and Applications

Springer

Advanced Structured Materials

Volume 5

For further volumes:
http://www.springer.com/series/8611

Noorhana Yahya

Carbon and Oxide Nanostructures

Synthesis, Characterisation and Applications

Springer

Assoc. Prof. Dr. Noorhana Yahya
Department of Fundamental and Applied Sciences
Universiti Teknologi PETRONAS
Bandar Seri Iskandar
31750 Tronoh, Perak
Malaysia
noorhana_yahya@petronas.com.my

ISSN 1869-8433
ISBN 978-3-642-14672-5 e-ISBN 978-3-642-14673-2
DOI 10.1007/978-3-642-14673-2
Springer Heidelberg Dordrecht London New York

Library of Congress Control Number: 2010937766

Cover design: WMXDesign GmbH, Heidelberg, Germany

Printed on acid-free paper

Springer is part of Springer Science+Business Media (www.springer.com)

Preface

It is my privilege as the Editor-in-Chief to present to you an effort of our team of prominent contributors to this monograph on Carbon and Oxide Nanostructures. Over the past 20 years, carbon and oxide nanostructures evolved into one of the most studied objects and are presently entering in the transition phase from nanoscience to nanotechnology. Carbon and oxide nanostructures constitute an enormous topic which may only be described in a simplified manner, which in essence is the intent of this book. It is hoped that this book would provide valuable resources for researchers as well as postgraduate students of physics, chemistry and engineering. Related carbon-based materials such as fullerenes, carbon fiber, glassy carbon, carbon black, amorphous carbon, diamond, graphite, buckminsterfullerene, and carbon nanotubes (CNTs) are discussed. CNTs which have attracted the attention of the scientific community due to their fundamental and technical importance are elaborated. It also presents a review of the applications of fullerene and its derivatives as electron beam resists, as well as outlining the effects of catalyst on the morphology of the carbon nanotubes. Structural and optical properties of hydrogenated amorphous carbon (a-C:H) thin films prepared in a DC-plasma-enhanced chemical vapor deposition reactor is discussed in greater detail. Some of the works done on polymer-CNTs-based solar cells with a variety of device architecture and band diagram are summarized. Several irregular configurations of carbon nanofibers (CNF) such as coiled, regular helical, and twisted coil are elaborated. This book also includes the molecular modeling of carbon-based nanomaterials including discussions on some aspects of the issues related to the synthesis and characterization of diamond prepared via CVD techniques using the hot filaments and plasma. Oxide-based materials related to fuel synthesis and solar hydrogen production are also presented. The versatility of ZnO nanostructures and some of the novel applications such as solar cells and light-emitting devices are being highlighted. A brief introduction of Fe–FeO nanocomposites and some superparamagnetism studies in the form of particles and thin films are included. The benefits and drawbacks of the properties of some nanomaterials used in optical sensing applications are given, and the recently developed optical chemical sensors and probes based on photoluminescence are also rigorously overviewed. Aspects of nanocatalytic reactions, the types of catalyst, and also the preparation and characterization of the active catalyst for ammonia synthesis are scrutinized.

I am grateful to all authors who have contributed to the chapters of this book. All merits on overview of such an enormous topic as Carbon and Oxide Nanostructures in this concise monograph should be credited to all contributing authors, but any shortcomings to be attributed to the Editor-in-Chief. The book is dedicated with all sincerity to all whose work has not received due reference and recognition.

Universiti Teknologi PETRONAS Assoc. Prof. Dr. Noorhana Yahya
Malaysia

Contents

Carbon Nanotubes: The Minuscule Wizards 1
Noorhana Yahya and Krzysztof Koziol

Synthesis of Carbon Nanostructures by CVD Method 23
Krzysztof Koziol, Bojan Obrad Boskovic, and Noorhana Yahya

Fullerene (C60) and its Derivatives as Resists for Electron Beam Lithography 51
Hasnah Mohd Zaid

Hydrogenated Amorphous Carbon Films 79
Suriani Abu Bakar, Azira Abdul Aziz, Putut Marwoto, Samsudi Sakrani, Roslan Md Nor, and Mohamad Rusop

Carbon Nanotubes Towards Polymer Solar Cell 101
Ishwor Khatri and Tetsuo Soga

Irregular Configurations of Carbon Nanofibers 125
Suriati Sufian

Molecular Simulation to Rationalize Structure-Property Correlation of Carbon Nanotube 143
Abhijit Chatterjee

Carbon Nanostructured Materials 165
Azira Abdul Aziz, Suriani Abu Bakar, and Mohamad Rusop

Diamond: Synthesis, Characterisation and Applications 195
Roslan Md Nor, Suriani Abu Bakar, Tamil Many Thandavan, and Mohamad Rusop

Versatility of ZnO Nanostructures 219
Muhammad Kashif, Majid Niaz Akhtar, Nadeem Nasir, and Noorhana Yahya

Supported Nanoparticles for Fuel Synthesis 245
Noor Asmawati Mohd Zabidi

Nanotechnology in Solar Hydrogen Production 263
Balbir Singh Mahinder Singh

Fe–FeO Nanocomposites: Preparation, Characterization and Magnetic Properties 281
Jamshid Amighian, Morteza Mozaffari, and Mehdi Gheisari

Nanostructured Materials Use in Sensors: Their Benefits and Drawbacks 307
Aleksandra Lobnik, Matejka Turel, Špela Korent Urek, and Aljoša Košak

Zinc Oxide Nanostructured Thin Films: Preparation and Characterization 355
Mohamad Hafiz Mamat and Mohamad Rusop

Superparamagnetic Nanoparticles 375
Boon Hoong Ong and Nisha Kumari Devaraj

Ammonia Synthesis 395
Noorhana Yahya, Poppy Puspitasari, Krzysztof Koziol, and Pavia Giuseppe

Diamond: Synthesis, Characterisation and Applications

Roslan Md Nor, Suriani Abu Bakar, Tamil Many Thandavan, and Mohamad Rusop

Abstract In this chapter we review some aspects of the synthesis and characterisation of chemical vapor deposited diamond. Chemical Vapor Deposited (CVD) diamond is arguably the first of the "new" carbon materials that has received extensive research attention due to its potential industrial applications. Intense research activities on CVD diamond that spanned over 30 years brought much progress in understanding and techniques on the synthesis and laboratory demonstration of applications. However, industrial scale applications are still elusive, mainly due to the many technical hurdles that must be overcome in order to fully benefit from the wonderful properties of diamond. Although CVD diamond has been superseded by fullerene in the 1990s, later carbon nanotubes and more recently the emergence of graphene, it is worth looking at this fascinating form of synthetic diamond which may yet make a comeback in years to come. Attention was given to the established techniques for the synthesis and characterisation of CVD diamond as well as issues related to the challenges of industrial applications of CVD diamond.

R.Md. Nor (✉) and T.M. Thandavan
Department of Physics, Faculty of Science, University of Malaya, 50603 Kuala Lumpur, Malaysia
e-mail: rmdnor@um.edu.my

S.A. Bakar
NANO-SciTech Center, Institute of Science, Universiti Teknologi MARA, 40450 Shah Alam, Selangor, Malaysia

Faculty of Electrical Engineering, Solar Cell Laboratory, Universiti Teknologi MARA, 40450 Shah Alam, Selangor, Malaysia

Physics Department, Faculty of Science and Technology, Universiti Pendidikan Sultan Idris, 35900 Tanjung Malim, Perak, Malaysia
e-mail: absuriani@yahoo.com

M. Rusop
NANO-SciTech Center, Institute of Science, Universiti Teknologi MARA, 40450 Shah Alam, Selangor, Malaysia
Faculty of Electrical Engineering, Solar Cell Laboratory, Universiti Teknologi MARA, 40450 Shah Alam, Selangor, Malaysia
e-mail: rusop8@gmail.com

N. Yahya (ed.), *Carbon and Oxide Nanostructures,* Adv Struct Mater 5,
DOI 10.1007/8611_2010_17,
Published online: 6 July 2010

1 Introduction

Carbon is the only element in the periodic table that has four isomers from 0 dimensions to 3 dimensions. There are two well known polytypes, namely graphite with sp^2 hybridized bond and diamond with sp^3 hybridized bonds. During the last 30 years, a number of "new" carbon forms have received vast attention, all of which are variations of the two forms of carbon mentioned above. The "new" carbon forms are CVD diamond [1–3], which is the subject of this chapter, fullerenes, carbon nanotubes and graphene.

Fullerenes are a class of carbon materials with 0 dimensions which were first discovered in molecular beam experiments in 1985 by Harold W. Kroto, Robert F. Curl and Richard E. Smalley [4]. The most abundant of the fullerenes is C_{60}. It has the structure of hollow spherical cluster of 60 carbon atoms forming a complete molecule. In each molecule, 12 pentagons associated with sp^3 hybridization and 20 hexagonal formation of carbon atoms involving sp^2 hybridization [5, 6], joined together to form a complete spherical shape.

Carbon nanotubes were first discovered in 1991 created much attention as one dimensional nanostructured pure carbon materials with numerous useful properties which are of interest to both industrial applications and fundamental research [7]. The latest of the new carbon material is graphene which is one atom thick layer of two-dimensional carbon atoms with sp^2 bonding. Theoretical speculation have long showed that a single layer graphene sheet should be thermodynamically unstable but this was dispelled in 2004, when it was first fabricated by mechanically cleaving of Highly Oriented Pyrolytic Graphite (HOPG) [8].

2 Diamond

Diamond has been revered by humans since ancient times mainly as gemstone. Its scarcity, hardness and bright sparkle makes it a status symbol. Apart from being the much sought after gemstone, the many remarkable properties of diamond have similar appeal to material scientists and engineers. Among the properties are hardest known material, chemical inertness, and highest thermal conductivity at room temperature, least compressible and highest stiffness. When doped, diamond exhibit semiconducting properties with a larger band gap of 5.4 eV which can be useful for the fabrication of microelectronics devices for high frequency and high power applications.

Diamond which is carbon in the most concentrated form, involves sp^3 hybridization of the valence electrons in carbon to form chemical bonds. In diamond each carbon atom shares all four of its available electrons with adjacent carbon atoms, forming tetrahedral unit, with 1.54 Å in length [9]. This shared electron-pair bonding forms the strongest known chemical linkage, sp^3 hybridized electrons forming the covalent bond, which is responsible for the many superlative properties

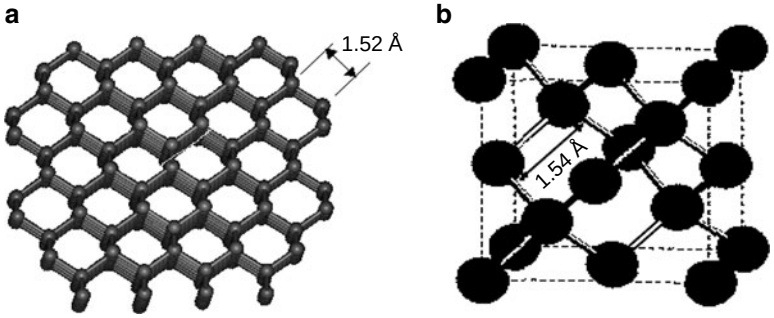

Fig. 1 (**a**) Diamond lattice (**b**) Face-centered cubic structure of diamond

of diamond. This bond form equal angles of 109°28′ separating each carbon atoms. The repeating structural unit of diamond consists of eight atoms, which are fundamentally arranged, in a cube [10] as shown in Fig. 1.

With this cubic form and its highly symmetrical arrangement of atoms, diamond crystals can develop in a variety of different shapes known as 'crystal habits'. The octahedron shape is the most common crystal habit. But diamond crystal can also form cubes, dodecahedra, and even combinations of these shapes.

2.1 Natural Diamond

Diamonds were first mined in India as early as 4,000 years ago. Up to until the eighteenth century mines of Golconda in India were the only known market for the trade of gemstones diamond. Then Brazil became the main producer after diamonds were found there in 1726. Later in 1867 diamond was discovered in Hopetown, South Africa [11], which up to this day remained a major supplier.

Natural diamonds were thought to be created under extreme conditions due geological processes at more than 150 km in the mantle of the earth. The diamond crystals formed were then transported to the surface of earth in molten rock, or magma in explosive volcanic eruptions. Although diamonds are not formed near the earth's surface, where graphite is the preferred stable form of carbon, some diamonds formed in extreme conditions in the crust of the earth survived at the surface because a temperature of about 600°C is required to decompose diamond to carbon dioxide.

2.2 Synthetic Diamond

Today, synthetic diamond can be fabricated using two different methods, with different conditions. The earlier and more established method was the High

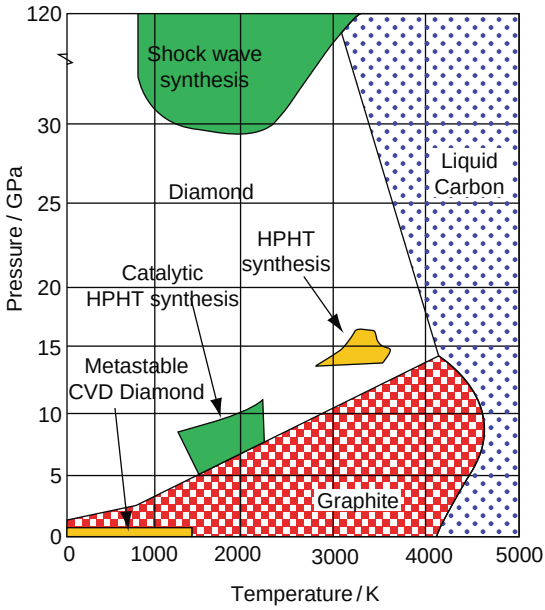

Fig. 2 Phase diagram of carbon [13] – gives a short description of how the phase-diagram was constructed from experimental data and calculations

Pressure High Temperature (HPHT) technique which duplicates the condition of natural diamond formation [9]. Using the HPHT technique synthetic diamond can be converted directly from graphite under specific conditions. At present, synthetic diamond formed using the high pressure high temperature technique is a major source of industrial diamond, mainly as abrasives and drill bits [12]. Alternatively, the Chemical Vapour Deposition (CVD) technique is the method to synthesis diamond at low pressure and low temperature conditions from gas phase precursors. The main attraction of CVD diamond is its film form where new potential applications such as coatings or optical mirrors are possible. The possibility of CVD diamond synthesis was first proposed in 1955, when Bundy et al. [13] presented the carbon phase diagram as illustrated in Fig. 2. The diagram shows the thermodynamic stability for graphite and diamond at different temperatures and pressures. The position of the diamond/graphite equilibrium line was established by thermodynamic calculations based upon the measured physical properties of graphite and diamond in the temperature range from 300 to about 1,200 K and by experiments on growing or graphitization of diamond. It has been proposed that a temperature, pressure phase diagram for carbon which included a wide temperature, pressure area at lower pressures and temperatures in which there would be in apparent equilibrium state or 'pseudo-equilibrium' between diamond and graphite [14]. The quantitative of free energies of graphite and diamond determination by Rossini et al. showed that their difference at one atmosphere, 0 K, is only about 2.5 KJ mol^{-1} [15].

2.3 High Pressure High Temperature (HPHT) Diamond

The carbon phase diagram illustrated in Fig. 2 shows that diamond is unstable with respect to graphite except at high temperatures (>1,300°C) and high pressures (>40 kbar).

In 1955, H. T. Hall and co-workers at General Electric developed the solvent-catalytic HPHT method [13, 16]. In this procedure graphite was compressed in a hydraulic press in the presence of a suitable molten metal catalyst/solvent until carbon dissolved and diamond crystallized. Sufficiently high temperature was provided by passing an electric current through the sample. Molten metals like Ni, Co or Fe are commonly used which dissolve graphite at elevated pressures of between 5 and 10 GPa, and temperatures in the range of 1,300–2,300°C. The dissolved carbon re-crystallizes into diamond at normal pressures and temperatures. The transition of graphite to diamond is accompanied by volume decrease of 43%, posing severe technical problems to maintain suitable pressure, being a vital condition [17]. If the pressure is not maintained, the formed diamond would convert itself back to graphite immediately. Synthetic diamond crystals with sizes ranging from few nanometres to millimetres were recovered from the process by dissolving the metal catalysts in acid [18].

There are applications of HPHT diamond materials. Diamond grit are used as cutting tool in industries and the main bulk of diamond used here are synthetic more viable than the use of natural diamond. Russell Hemley at Carnegie institution had found that most HPHT synthetic diamond is yellow and most CVD diamond is either milky white or greyish, limiting their optical applications. Colourless diamond are costly to produce using the HPHT method and this situation had limits the general applications of these diamonds as gems, in optics, and in scientific research. CVD diamond which is grown under non-thermal equilibrium conditions can be stable even at low pressure [19]. CVD diamond which can be produced in film form at this condition has similar properties as natural diamond and therefore provided tremendous prospective applications in industry.

2.4 Low Pressure Low Temperature CVD Diamond Synthesis

The notion of growing diamond from gas at pressures lower that atmospheric and temperatures lower than 1,000°C may seem counter intuitive, but the mechanism involved is totally alien of the HPHT process. The first reported success of low pressure low temperature was reported by Eversole in 1962, whereby the optimal temperature and pressures were 900°C and 0.1 Torr respectively [20]. In a patent they described a cyclic process for hydrocarbon pyrolysis onto a diamond surface followed by a separate graphite etching step using H atoms.

This was extended by Derjaguin et al. from the Soviet Union [10]. They performed a physical chemistry experiments such as thermal gravimetric analysis

(TGA) to observe weight gain in diamond powder with complete removal of residual graphite, from a CVD synthesis. They were partially successful in producing epitaxial films growth at a slow which was not completely free of graphitic carbon. These initial works demonstrated the feasibility of CVD diamond synthesis, albeit on a diamond substrate.

In 1968, Angus [21] showed that synthetic diamonds were identical with natural diamond and later showed that semiconducting diamond can be obtained by doping diamond grown from methane and hydrogen with boron [22, 23]. Japanese scientists at the National Institute for Research in Inorganic Materials (NIRIM) in Japan developed various diamond thin film deposition techniques such as CVD with the activation of carbon-containing gases, physical vapour deposition (PVD) from a solid carbon source and hybrid processes involving solids, carbon and catalytic materials and gases as the sources. These were done both on diamond or non-diamond substrates. Generation of atomic hydrogen near deposition surface was found to be the major common factor in diamond growth [11].

3 Mechanism of CVD Diamond Growth

Chemical vapor deposition refers to the process where solid materials are formed from the gas phase at some suitable temperature and pressure. Figure 3 shows a schematic diagram demonstrates the chemistry of hydrocarbon radicals and

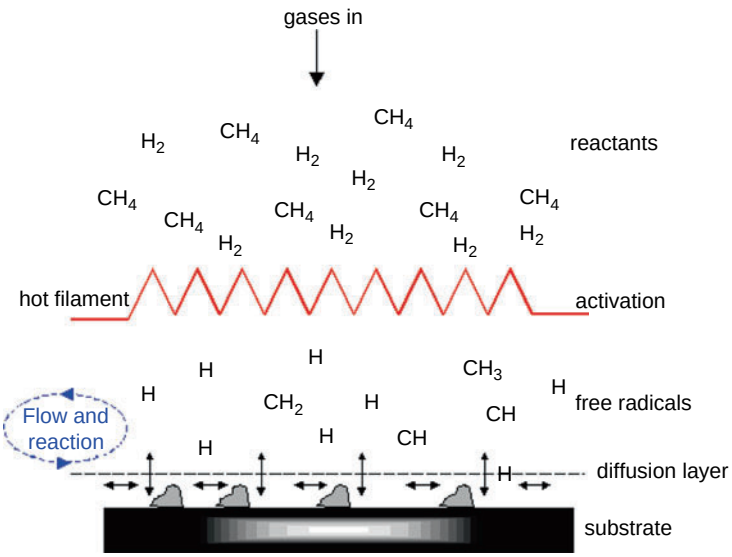

Fig. 3 Chemistry of hydrocarbon radicals and hydrogen atoms in a hot filament chemical vapor deposition method

hydrogen atoms generation in a hot filament, representing typical diamond CVD environment.

Synthesis of CVD diamond would involve some carbon containing gas (CH_4, C_2H_2) diluted in hydrogen. The precursor gas would not readily condense on the substrate to form diamond. A mechanism to dissociate the gas to generate active species such as CH_3, CH_2, CH, and C are necessary. One of the most common techniques is using a hot filament, where the gas molecules are thermally dissociated.

Typically the reactant gas mixture, for example low concentration of CH_4 in H_2 is introduced into an evacuated reactor chamber trough a hot filament above a substrate. With filament temperatures reaching 2,000°C, CH_4 and H_2 are decomposed upon collision on the surface of the hot filament wire to produce a variety of hydrocarbons radicals and H atoms.

The radicals then reacted chemically either in gaseous phase or on selected substrate materials. The general opinion is that the hydrocarbon methyl radical CH_3 is the main growth species in a CVD growth condition [24–26]. To picture this simplistically, in a deposition environment, CH_3 radical diffuses to substrate surface and is deposited on an active surface site, retaining its tetrahedral form with the three hydrogen atoms sticking away from the substrates. The hydrogen atoms can be removed from the surface by H atom to form H_2 or a CH_3 radical to form CH_4, leaving a dangling bond to receive another CH_3 radical or to form bridging bond with another surface carbon atom. The process will continue, building up the diamond nucleus with the addition of CH_3 radicals and the removal of surface H atoms and the addition of CH_3 radical to dangling bonds on the surface.

Other active species such as CH_2, CH and C although at a much lower concentration at the substrate surface, contributed to the growth of diamond [27]. The CH_2 radical upon condensation on the surface have a dangling bond ready for the addition of another radical or for bridging bond with another carbon atom on the surface. Similarly, the condensation of CH and H radicals may lead to carbon with diamond structures based on similar processes of addition and abstraction of actives radicals.

The chemistry of hydrocarbon species and hydrogen atoms has already been studied by many researchers and scientist in the past 10–15 years ago. Bachmann et al. [27] introduced the first C H O phase diagram providing a common scheme for all major diamond chemical vapor deposition (CVD) methods used to date. They had discovered that at low pressures, good quality diamond films can be synthesized from different gas mixtures by thermal CVD, Hot Filament CVD, combustion flames and various plasma deposition techniques.

3.1 Choice of Substrate for Diamond Growth

It is most desirable to deposit diamond on any substrate of choice. However, there are many restrictions. Ferrous metals are unsuitable due to the high solubility of

carbon. Materials with melting points lower that the deposition temperatures are also not suitable.

For good adhesion the selected substrates are required to have a comparable thermal expansion coefficient with natural diamond which is 1.18×10^{-6} K^{-1} [28]. This is important because the substrate will expand at the high temperature and during deposition and upon cooling to room temperature; the substrate and the diamond film will contract unevenly and at different rates due to the different coefficient of expansions resulting in compressive or tensile residual stresses which could lead to cracks and delaminating of diamond film. For homoepitaxial growth, another consideration is the matching of the lattice of the substrate with that of diamond. This condition, while not affecting the growth of diamond can significantly affect adhesion of the diamond film to the substrate.

The most efficient substrate is diamond itself. Silicon is the next most efficient and the most studied substrate for CVD diamond growth. The lattice mismatch between silicon and diamond is about 52% where the lattice constant of silicon is 5.4301 Å and for diamond is 3.5667 Å. Furthermore, there a large difference in the coefficient of thermal expansion where for silicon it was two orders of magnitude smaller at 2.1×10^{-8} K^{-1} [29]. Despite these differences, efficient growth of CVD diamond with good adhesion to silicon substrates was routinely reported. The reason for this was that the growth of diamond was not directly on the silicon substrate but on a carbide layer formed prior to diamond nucleation [30]. Similarly, other carbide forming metals such as molybdenum, tungsten and titanium, and the carbides of this metal have been utilized as substrates. The degree of adhesion varied with different materials where the fabrication of free standing CVD diamond would favor substrates with the least adhesion. The effect of carbide formation can be demonstrated with the aid of Fig. 4, which shows the XRD spectra of CVD diamond on silicon and molybdenum substrate deposited using the MWPCVD at different temperatures. Notice that significant carbide formation is evident in the sample on molybdenum, which inevitably affect adhesion of the diamond film.

3.2 Substrate Pretreatment Methods and Diamond Nucleation

CVD diamond formation on non-diamond substrates occur by a two steps mechanism, that is, nucleation of diamond seeds and further growth of diamond on the seeds. The efficiency of the nucleation in terms of density and quality will inevitably influence the growth rate and morphology of the film. The nucleation process occurred in a carbon saturated state which facilitated the nucleation process [23]. The initial surface condition of substrate material is very important for diamond nucleation and growth rate. Even with silicon, the strongly favored substrate material, diamond nucleation is very poor on mirror-polished silicon substrates [31]. Therefore pretreatment of substrate are commonly applied to enhance diamond films growth on silicon.

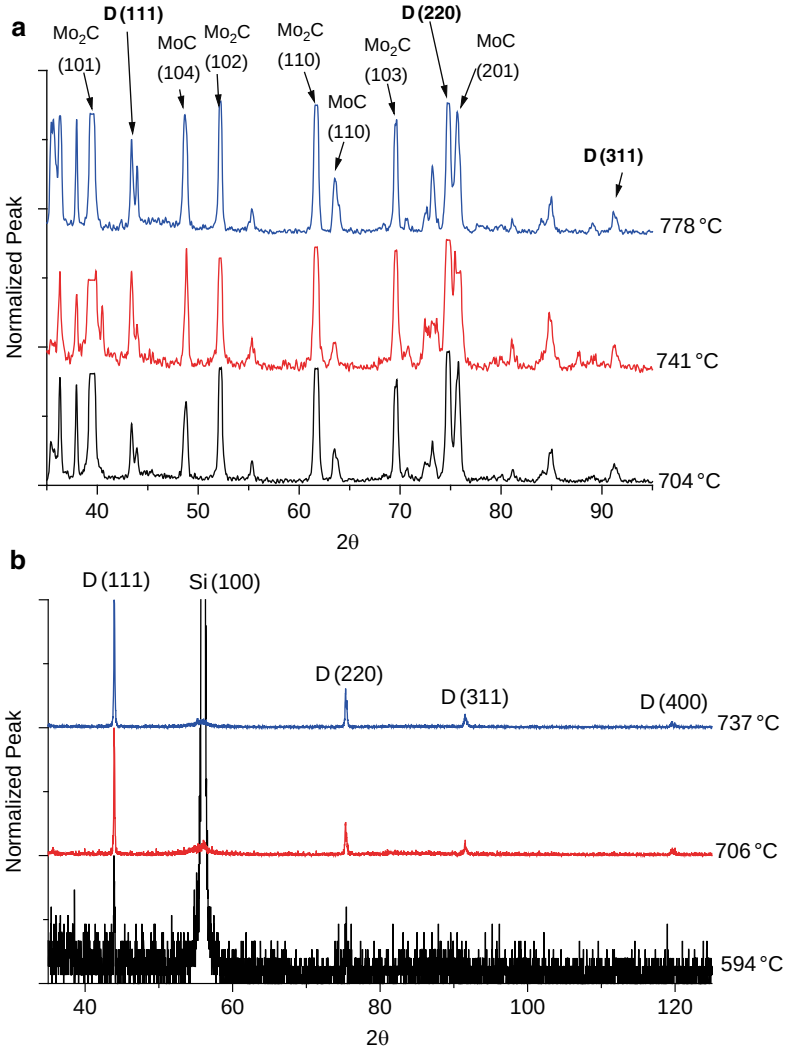

Fig. 4 XRD spectra of CVD diamond deposited at different temperatures on (**a**) Silicon substrates (**b**) molybdenum substrates. Notice the rich carbide peaks in the diamond sample on the molybdenum substrate

The nucleation density of diamond could be significantly enhanced by scratching or abrading the silicon substrate surface with micrometer sized diamond abrasive [32, 33], SiC sand paper [34], cubic BN [35] and stainless steel paste [36]. Among these abrasives, diamond pastes gave the best nucleation density and subsequently the best growth rates. This phenomenon is demonstrated with the aid of Fig. 5 which shows the SEM micrographs showing the effect of scratching on the nucleation of

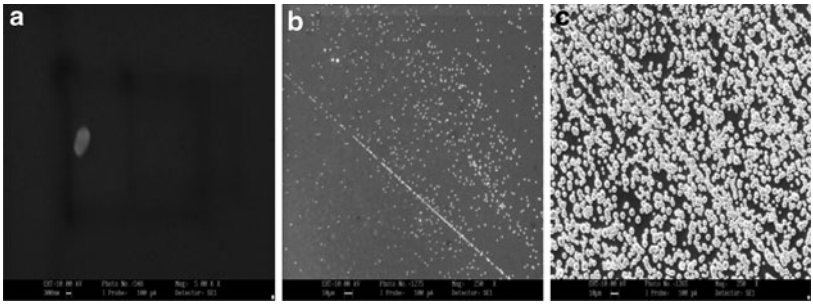

Fig. 5 Effect of scratching the substrate surface (silicon) with (**a**) unscratched (**b**) sand paper (**c**) SiC abrasive (**d**) diamond particle (15 μm)

CVD diamond grown using the microwave plasma deposition technique. Here, three mirror polished Si (100) substrates, the first was unscratched (Fig. 5a), second scratched with SiC abrasives (Fig. 5b) and the third with diamond particles of average grit size of 15 μm (Fig. 5c) were compared. Deposition was done on all three substrates simultaneously to keep the conditions similar. It is evident from the SEM micrographs that scratching Si surface with diamond significantly enhanced the nucleation of diamond, both in terms of quality and quantity. Notice that there were preferential growth in the scratch lines of the substrates abraded with SiC (Fig. 5b) and diamond grits (Fig. 5c).

This phenomenon can be explained as follows. Scratching removes atoms from the surface and leaves behind dangling bonds which are active sites for hydrocarbon radicals to react and condense on. When scratched with diamond abrasives, some of the nanosized diamond fragments may be trapped on the silicon surface and acts as seeds for efficient diamond nucleation and enhancement of growth. The formation of grooved lines facilitated turbulent flow of the precursor gas during deposition which somehow promoted nucleation of diamond on silicon.

Alternative techniques such as ion beam sputtering to create sub-micrometer scale craters using focused 25 keV Ga^+ beams [37], etching in KOH to create micrometer scale *V* grooves [38], coating with hydrocarbon oil of a low vapor pressure and high thermal stability [39], coating with thin layer of evaporated carbon [40], applying substrate bias voltage [41, 42] and 25 keV Si^+ ion beam implantation [43] are some of the pretreatment methods that have been applied to enhance the nucleation of diamond films. Yang et al. [44] had reported that ion implantation did not make substrate surfaces as rough as mechanically scratched or chemically etched process but still enhanced nucleation.

It is believed that by applying pretreatment process on silicon substrate, the resulting surface stresses have some influence on diamond nucleation. The surface energy of the substrate may increase due to an atomic displacement process which influences the diamond growth process. It is also possible that surface treatment cause reduction in the surface energy difference between Si and diamond enhance

the nucleation. Pretreatment process allows changes in surface morphology because it favors the formation SiC which functioned as the diamond growth layer [44].

In a conventional method of hot filament chemical vapor deposition environment most of the species are neutral and positively and negatively charged species are present with different number density and with the overall density expected to be very much less than, for example, in a microwave plasma [45]. Electrically biasing silicon substrates during deposition, using either negative or positive voltage has been shown to be effective in enhancing nucleation rates. In the case of negative bias voltage, the effect may be attributed to a sputtering effect due to an increase in the kinetic energy of incident positive ions. When the substrate is positively biased negative ions and electrons bombard the substrate surface to bring about sputtering and the creation of active nucleation sites.

George et al. [45–47] reported that negative bias definitely enhances the amount and crystalline of the deposits which was identified by XRD and AFM studies. Cui and Fang [48] have reported that biasing influenced the distribution of hydrocarbon species and the electron temperature. They reported that nucleation density increased by a factor of two at a 120 V bias meanwhile at 200 V it was enhanced more than an order of magnitude. Sawabe et al. [49] found that positive biasing method can enhance nucleation density and Chao et al. [50] observed that with positive bias much smoother surface was obtained. This can be due to the significantly small number densities of negative ions, so that the surface was essentially bombarded by electrons which resulted in surface activation with little damage. Stoner et al. [51] reported that negative biasing in MWCVD have also increased the nucleation density of diamond. An investigation of DC and AC bias voltage by Kromka et al. outlined some interesting features [52]. At higher DC bias voltage degradation of nucleation process was reported compared to low DC bias voltage which was due to excessive sputtering during the deposition process. In AC bias voltage higher voltage is required to obtain dense packed and well-faceted diamond grains.

A slight increase of hydrogen atom percentage with biasing are not expected to affect the gaseous component mean temperatures and hydrocarbon species concentration distributions. However, methane and hydrogen decomposition can be accelerated by electron bombardment adding growth species and H atoms to enhance nucleation. Although the electron density depends on the filament temperature, the numbers of electron impinge on substrate surface will be increased due to biasing and create active sites for nucleation. In another study, Mahajan et al. reported coated SnO_2 on silicon substrates and observed nucleation density increased irrespective of whether the substrate surface is pretreated or not, prior to SnO_2 deposition [53]. The issue enhancing of nucleation density of CVD diamond is still unresolved. Although many published reports have provided some understand basic underlying mechanisms, a truly efficient technique have yet to be developed for industrial scale production of CVD diamond. Furthermore, nucleation enhancement may be influenced by the formation of diamond structured stable clusters of from hydrocarbon in the gas phase which condensed on the substrate surface as preferred nucleation sites [54].

3.3 The Role of Atomic Hydrogen in CVD Diamond Growth

As mentioned earlier atomic hydrogen (H) is one of the key constituent in the growth of CVD diamond. They were produced heterogeneously by the decomposition of hydrogen gas (H_2).

$$H_2(g) \rightarrow H + H \tag{1}$$

The condensation of all the carbon containing radicals basically adds carbon to the substrate surface. It is well known that the formation of non-diamond carbons (graphite and amorphous carbon) is much more efficient than that of cubic diamond. The atomic hydrogen formed preferentially etches sp^2 graphite and amorphous carbon at a much higher rate than diamond [55–57]. Another important role of hydrogen atom is to stabilize the growing sp^3 bonded carbon on the substrate whereby resulting in surface termination which prevented cross-linkage, and subsequent reconstruction of the surface to graphite. During deposition dangling bonds might be created by thermal desorption and abstraction of the surface hydrogen atoms. Thus a large number of reactive hydrogen atoms are required to make bonds to the excess dangling bonds, avoiding surface graphitization. Spatial distribution of atomic hydrogen is strongly dependent on parametric conditions [57].

Atomic hydrogen accelerates the gas phase reaction and promotes the decomposition rate of CH_4 or C_2H_2 into active radicals.

$$CH_4 + \bullet H \rightarrow CH_x + H_2 \quad (x = 1 \text{ to } 3) \tag{2}$$

$$C_2H_2 + H \rightarrow C_2H + H_2 \tag{3}$$

4 Plasma Enhanced Techniques for Chemical Vapour Deposition Diamond Synthesis

4.1 Microwave Plasma Enhanced CVD (MWPECVD)

Scientists at the National Institute for Research in Inorganic Materials (NIRIM), Japan, demonstrated the first working microwave plasma enhanced CVD diamond system [58] where polycrystalline diamond growth was demonstrated on a silicon substrate. It is known that molecules are efficiently dissociated in microwave plasmas giving rise to a cocktail of neutral and charged particles as well as electron. The generation of plasma in a microwave system involves the oscillation of charged particles at the microwave frequency. Collision of electrons with gas atoms and

molecules generates high ionization fractions. Microwave plasmas are typically described as having "hot" electrons and "cool" ions and neutrals where the electron temperature can be in the hundreds of eV but the ions are essentially at room temperature. Under such conditions, high flux of energetic electrons on the substrate surface functioned as growth activators as a result of active sites formed.

Microwave energy is introduced into the reaction chamber using antennas or wave guides which convert a rectangular microwave signal into a circular mode, later pass through a silica microwave window (vacuum barrier) into a cylindrical cavity which is a PECVD process chamber. The location of the luminous plasma ball is controlled by the cavity tuning as well as the pressure, power, and gas phase composition of plasma. The luminous ball will further contract in size as the pressure in the chamber increases. The luminous ball will increase in diameter as the microwave power is increased.

This technique of plasma generation exhibits good stability and high density plasmas and the generation of the plasma does not require any electrode, thus eliminating the possibility of contamination from particles sputtered from the electrode. The plasma is also confined to the center of the deposition chamber to form ball-shaped plasma, thus carbon deposition on the walls of chamber is minimal. The main disadvantage the MWPECVD is the difficulty of scaling up to industrial scale.

4.2 Direct Current (DC) Plasma Enhanced CVD

In DC plasma CVD, a negative or positive DC voltage is applied to the substrate platen or to an auxiliary electrode to generate plasma in rarefied gas mixture. Intermediate electrodes may be used to guide the plasma and to alter the plasma position and properties. DC plasma enhanced CVD shows both advantage and disadvantage. The diamond deposition area is only limited by the size of the electrodes and the DC power supply which is technically relatively easy to overcome. The disadvantage of DC plasma enhanced CVD is that it may self extinguish if a very thick film is grown since a biased platen will change its bias if coated by a dielectric diamond film.

Japanese scientists developed the DC arc PECVD methods which created thermal plasmas capable of growing diamond films at rates $\geq$20 μm h^{-1}. Kurihara et al. at Fujitsu Laboratories have developed a DC plasma jet process called the DIA-jet process [59] which utilized a gas injection nozzle composed of a rod cathode concentric with a tube anode. Gases passed between the cathode and anode and were sprayed out from an orifice in the anode. The gas mixture is CH_4 and H_2 with a carrier gas (Argon or Helium); the total pressure is between 4.1 and 41 kPa (30–300 torr) were typical. The DC arc is sustained by 80–150 V and 10–50 A (power of 0.8–7.5 kW); the substrate was water cooled to maintain the substrate temperature between 520 and 1,220°C. Typical growth rates reported to be as high as 80 μm h^{-1}. DC arc methods have demonstrated high deposition rates and ability to

synthesize high quality diamond and are gaining acceptance as a commercially viable manufacturing technology for diamond film synthesis; De Beers's industrial diamond developing CVD diamond using 10 kW DC Arc jet system.

4.3 Radio Frequency Plasma Enhanced CVD

Radio Frequency plasmas are widely used in the fabrication of silicon based microelectronics mainly in dry etching systems. As a result, rf plasma systems technology are the most developed. There have been sparse reports on the use of rf plasma to fabricate diamond thin films. In most reports, inductively coupled rf plasmas were used since these are simple systems capable of generating high density plasmas. Furthermore, rf power coupling to the gas using conductive coils located outside the reactor chamber, thus eliminating contamination from sputtered coil materials. Rudder et al. [60] and Bozeman et al. [61] reported the deposition of CVD diamond using rf plasmas with the methane–hydrogen system and verified the existence of cubic diamond based on Raman spectroscopy and X-ray diffraction. Although existence of cubic diamond was proven, Raman spectra showed significant inclusion of graphitic carbon. Furthermore, less facetted diamond crystallites based on their SEM analysis again indicated the inclusion of graphitic carbon, at least on the surface. An important point reported was that diamond growth in an rf plasma was feasible at pressures >1 torr and high input power. Noda et al. [62] reported using ICP rf plasma to deposited diamond using methanol-hydrogen-water system at relatively low pressure of 80 mtorr. They reported enhanced diamond growth with increasing water partial pressure of up to 40 mtorr.

Studies by our group [63, 64] showed that significant silicon substrate damage occurred at pressures lower than 20 mtorr based on the observation of pits and no deposition. This is especially true when the plasma was operated in the H-mode where the plasma density is much higher than the E-mode. This is mainly due to the nature of inductively coupled rf plasmas which is high ion and electron temperatures. Furthermore, the formation of the sheath layer at the interface created significant electric field which gives kinetic energy to positive ions in the plasma. The ions impinge on the substrate surface as a consequent of its kinetic energy and also due to the fact the substrate is also more negatively charged that the environment, as a result of faster electrons. Ion temperatures of tens of eV and electron temperatures in the hundreds of eV are common in inductively coupled plasmas. Thus, the needs for higher pressures where ion and electron densities and temperatures are reduced due to gas phase collisions where diamond liked carbon are formed. Our study on a hybrid rf plasma and hot filament system showed that the effect of rf plasma activation and hot filament activation were independent of each other [65] where results from increasing rf power from 0 to 400 W reduced the amount of cubic diamond and enhanced graphitic carbon with increasing rf power. Excessive surface sputtering in the rf plasma due to the high density and energetic ion species seemed to be the main inhibitor of diamond growth.

5 Doping of CVD Diamond

The many excellent mechanical, chemical, optical and chemical properties of CVD diamond coupled with it is a material with a wide band gap makes it a prime candidate for specialized microelectronics materials. Being a material of negative electron affinity(NEA) conducting diamond films can function as robust field electron emitters, Doping with boron, which has an acceptor level of E_v +0.37 eV [66] has been investigated using the Cold Implantation Rapid Annealing (CIRA) technique [67]. Besides boron as a p-type dopant, n-type dopants like sulphur, lithium, sodium, and phosphorus were used in doping of diamond with varying degrees of success. The doping process can be done either during deposition (in situ doping) or post deposition (ex situ doping).

Li et al. [68] reported that in microwave plasma assisted CVD, sulphur incorporation was enhanced by the presence of boron but the donor level energy was reported to decrease from 0.52 to 0.39 eV. Borst and Weis investigated the electrical properties doped diamond film and found that Li, Na and P doped films had very high resistivity of over 10^9 Ωcm^{-1} [69]. They reported boron doped film showed activation energy of electrical resistivity in the range of 0–0.43 eV compared to 0.16 eV for lithium doped. Suzuki et al. [70] demonstrated that the p-type conduction existed for B doped CVD diamond based on (I–V) and (C–V) measurements. The barrier height Φ_b for the Schottky junction was reported to be 1.77 eV. They also reported the proportional increase of net acceptor concentration with boron concentration based on C–V measurements. Boron-doped CVD diamond electrodes fabricated by Latto et al. [71] showed that at an oxygenated electrode surface, two time constants were observed in impedance plots where the electron transfer process was thought to be mediated by surface states.

Bohr et al. [72] suggested that phosphorus addition during diamond growth influence the growth kinetics primarily due to surface reaction rather than to changes in the gas activation. They used 5% ultrapure phosphine 99.998% mixed in 94% hydrogen and 1% CH_4. Koizumi et al. [73] successfully fabricated phosphorus doped n-type diamond thin films with the activation energy of carriers at 0.46 eV in a higher temperature region and the Hall mobility was 28 cm^2 V^{-1} s^{-1} for a sample with 600 ppm PH_3 content in the deposition mixture. There has been report that increasing the amount of dopant source gas during diamond growth enhanced the growth rate for example, Tsang et al. reported enhancement with addition up to 2,000 ppm but decreased when PH_3 concentration reached above 3,000 ppm [74].

Sulphur doping in diamond film using the MWCVD system was reported by Petherbridge et al. [75]. They showed that sulphur incorporation into the diamond film are directly proportional to the H_2S concentration in gas phase at number densities about 0.2%. The sulphur incorporation was further supported by the four point probe measurement. The group compared HFCVD with MWCVD deposition of sulphur doping into diamond [76]. They reported little effect on film morphology or growth rate was observed for HF grown diamond films, even at high doping

levels (1% H_2S in the gas phase), and little or no evidence was seen for S incorporation into these films. In contrast, deposition from MW plasmas yielded diamond films of which the morphology, degree of S incorporation were strong variation of H_2S incorporation. Nishitani-Gamo et al. [77] reported producing sulphur doped homoepitaxial (001) diamond which showed n-type conduction by Hall Effect measurements in the temperature range 250–550 K. The mobility of electrons at room temperature was reported at 597 $cm^2\ V^{-1}\ s^{-1}$.

6 Characterization of CVD Diamond

One of the main issues related to the utilization of CVD diamond as an industrial material is the purity of the diamond film. As it is well known that sp^2 bonded carbon formation competes with the formation of diamond which is sp^3 bonded carbon. Here, we discuss three of the most common techniques, namely scanning electron microscopy, X-ray diffractometry and Raman spectroscopy.

6.1 Scanning Electron Microscopy (SEM)

Scanning electron microscopic images is undoubtedly the most appealing analysis technique when applied to CVD diamond. SEM gives the morphology of the crystal structure. For example, in Fig. 6, the crystal particle structure of CVD diamond deposited using the hot filament technique is clearly visible. Useful as it is in visually evaluating diamond film growth; the SEM technique by itself is inadequate in determining CVD diamond quality in terms of diamond and non-diamond composition of the sample. Well facetted crystal structures may harbor layers of amorphous carbon on its surfaces.

6.2 X-Ray Diffraction

X-ray diffraction method is one of the non destructive methods used for both lattice parameter measurement and crystallinity measurement. The phenomenon of X-ray diffraction by crystals results from a scattering process in which X-rays are scattered by the electrons of atoms without any changes in wavelength. A diffracted beam is produced by coherent or Bragg scattering only when certain geometrical conditions are satisfied. This may be expressed in either of two forms, Bragg's diffraction law or the Laue equations. From the Bragg equation for the cubic system

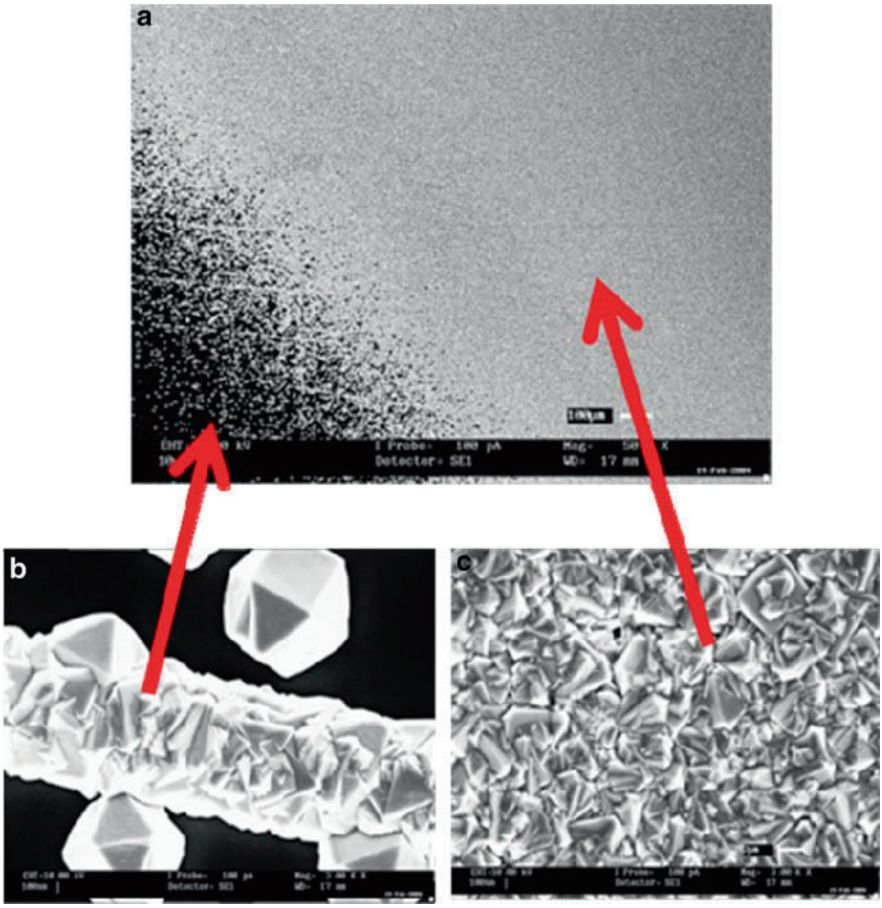

Fig. 6 Scanning electron microscopy (SEM) images (**a**) diamond film layer on silicon substrate (**b**) diamond crystal at the edge of film and (**c**) polycrystalline diamond film in the center position

$$n\lambda = \frac{2a}{\sqrt{h^2 + k^2 + l^2}} \sin\theta \tag{4}$$

$$n\lambda = 2d\sin\theta \tag{5}$$

where d equals to $a/\sqrt{h^2 + k^2 + l^2}$, is the inter-planar spacing, θ is the diffraction angle, n is an integer and λ is the incident wavelength. The h, k and l are the Miller indices of the peaks and a is the lattice parameter of the elementary cell.

Figure 7 shows typical X-ray diffraction spectra of CVD diamond where the crystalline nature of the films is evident. It is obvious that the film is polycrystalline and the peak high distribution can be compare to standard values for powder diffraction, which can reveal preferences in crystal orientation. Also, peak positions

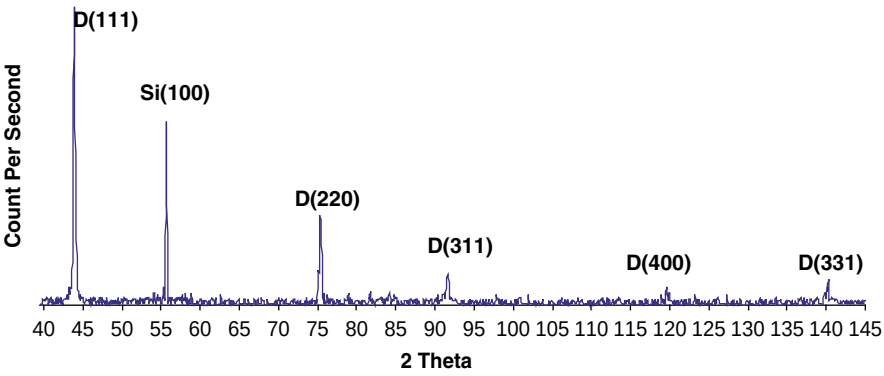

Fig. 7 Typical X-ray diffraction pattern of CVD diamond

which are normally shifted to higher or lower values than that of standards are signs of compressive and tensile stress respectively. Residual stress which is an important feature of CVD diamond on non-diamond substrates determines the adhesiveness of the film to the substrates. Studies using X-ray diffraction revealed that the main reasons can be attributed to lattice mismatch between diamond and substrate, and the difference in the coefficient of expansion of diamond and substrate materials.

In terms of elucidating the quality of CVD diamond, X-ray diffraction analysis has the capability to confirm the existence of crystalline diamond forms and to some extend crystalline graphitic carbon forms. The presence of amorphous carbon may not be efficiently detected.

6.3 Raman Spectroscopy

In the case of single crystal diamond, the carbon atoms are bonded to their neighbors by strong covalent sp^3 bonds, forming cubic structure belonging to the O_h^7 (Fd3m) space group. The diamond structure has only one triply generate optical mode at the centre of the Brillouin zone (T_{2g} symmetry) which appears as a sharp line at 1331.9 cm^{-1} [78]. Under ambient conditions, the graphite structure with strong in-plane sp^2 bonding is the most stable phase and the crystal structure belongs to the D_{6h}^4 (P63/mmc) hexagonal space group. The graphite crystal exhibits two Raman active modes, namely the E_{2g2} mode at 1,582 cm^{-1} and under special conditions, the E_{2g1} mode at 42 cm^{-1}.

The peculiarities of Raman spectra from CVD diamond can be demonstrated with aid of Fig. 7. For natural diamond, a sharp peak at about 1,332 cm^{-1} formed the signature for cubic diamond. The sharpness of the peak is due to symmetry of the carbon atoms bonded tetrahedrally in the diamond crystal. Typical spectra for CVD diamond shown in Fig. 7b illustrate a number of characteristics. Firstly, looking at the best diamond film which is the upper trace in Fig. 8b, there a

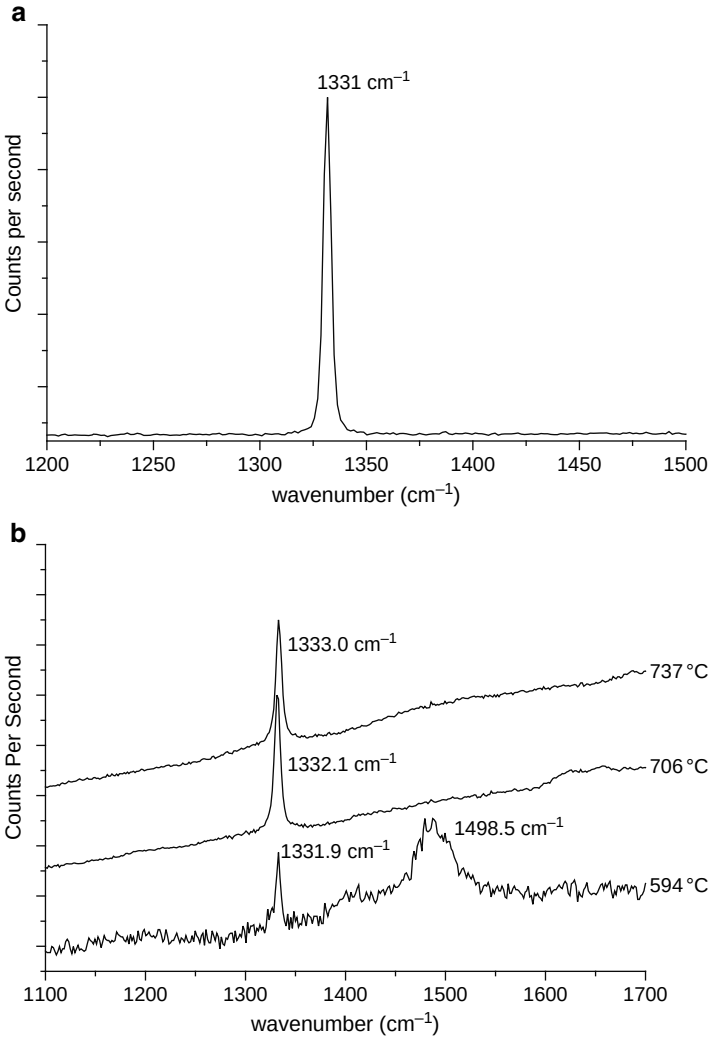

Fig. 8 Raman spectra of diamond (**a**) a clean spectrum from natural diamond (**b**) spectra obtained from CVD diamond synthesized using the microwave plasma technique on silicon substrates with 1% CH_4 and 99% H_2 at varying temperatures

luminescent background is evident. This was due to continuous emission as a result of crystal defects expected in CVD diamond. Another possible reason is due to the inclusion of impurity atoms, mainly nitrogen which is expected to be present in a CVD environment. By comparing the three spectra in Fig. 8b, it is clear that the film deposited at about 600°C significant peaks due to graphitic carbon around 1,400 cm^{-1} and 1,500 cm^{-1}. It is known that the Raman shift due to graphitic carbon is about 50 times more efficient than that of diamond [76], Raman

spectroscopy is an excellent technique for monitoring the presence of graphitic carbon in the film. Notice that the peak position of the diamond line increased with deposition temperature. This is due to the increase in the residual stress of films deposited at increasing temperatures, as a result of the difference between the values of the coefficient of expansion of diamond and silicon.

7 Potential Applications of CVD Diamond

Although it has been about 30 years the potential applications of CVD diamond have been enthusiastically promoted in numerous publications, grant submissions and talks it still remained in a potential. However it is worth a revisit and assesses the realities of these potentials. As mentioned earlier, the main strength of diamond as a material is it mechanical, chemical, optical and electrical properties. Optically diamond is transparent from the uv to the far infrared, making an excellent optical windows especially in hard environments. As medical radiation detectors, diamond is attractive because it is stable, non-toxic and atomic number value close to that of biological tissues. Vittone et al. [79] compared the thermoluminescence response of polycrystalline diamond with standard LiF TLD100 under beta irradiation and reported similar response for one of their diamond sample.

However, the most promising potentials are with conducting diamond films. Although, as microelectronics devices the issues related to wafer size single crystal fabrication and n-type doping still persist, applications in the field of electrochemistry seemed the most promising especially as electrodes for operations in harsh chemical environment. Such applications require the film just to be conducting without the stringent specifications of the electrical properties. Vinokur et al. has reported that boron doped diamond films exhibited unsurpassed properties for such applications [80].

Another promising application of doped diamond is as field electron emitters. However undoped diamond seemed to be more efficient emitters than conductive boron doped samples. This was attributed to emission from graphitic carbon present at the grain boundary of diamond particles in polycrystalline diamond samples [81].

8 Challenges of Industrial Scale CVD Diamond Production

After the much progress in the science and technology of the synthesis of CVD diamond the realization for actual industrial applications is still elusive [82]. The main obstacle remains the slow growth rate of a few μm per hour renders the process and the product too expensive. Furthermore, issues on the homogeneity of film quality remain an issue. Substrate surface temperature being a key parameter in the deposition process changed significantly after a layer of diamond is formed due to the high thermal conductivity of diamond. For the application of CVD diamond

as wear resistant coatings, serious issues related to substrate adhesion, substrate compatibility and residual stresses are still unresolved. Also, with the relatively high deposition temperature of present techniques most material surfaces are unsuitable for coating. As for potential applications for the fabrication of micro-electronic devices, two main technical hitches have to be overcome. Firstly, efficient and cheap techniques have to be developed to fabricate wafer size single crystal diamond. Secondly, these single crystal diamond wafers will have to be doped. While techniques of p-type doping mainly with boron have been quite developed, the progress in n-type doping still lags behind. Taking the silicon experience as a guide, many attempts on doping diamond with phosphorus have been reported but with no real breakthrough in terms of producing n-type diamond suitable for microelectronic devices. As such, the field of CVD diamond is still wide open waiting for a breakthrough for the excitement to return and possible some real industrial applications to be realized.

9 Summary

In this chapter some aspects of the issues related to the synthesis and characterization of CVD diamond is briefly revisited. CVD synthesis techniques using the hot filaments and plasma are discussed as demonstration for the CVD synthesis of diamond as a whole. Characterization of CVD diamond films based on evaluating film quality is discussed in the light of the scanning electron microscopy, X-ray diffraction and Raman spectroscopic techniques. The challenges of producing industrial scale CVD diamond was appraised in the light of technical difficulties highlighted by the numerous work during the golden age of CVD diamond.

References

1. Yarbrough, W.A., Messier, R.: Science **247**, 688–696 (1990)
2. Angus, J.C., Hayman, C.C.: Science **241**, 913–921 (1988)
3. Spear, K.E., Dismukes, J.P.: Synthetic Diamond: Emerging CVD Science and Technology. Wiley, New York (1994)
4. Saito, R., Dresselhaus, G., Dresselhaus, M.S.: Physical properties of carbon nanotubes. Top. Appl. Phys. (1998)
5. Saito, S., Oshiyama, A.: Phys. Rev. Lett. **66**, 2637–2640 (1991)
6. Zhu, X.D., Xu, Y.H., Naramoto, H., Narumi, K., Miyashita, A., Miyashita, K.: J. Phys. Condens. Matter **15**, 2899–2906 (2003)
7. Iijima, S.: Nature **354**, 56–58 (1991)
8. Novoselov, K.S., Geim, A.K., Morozov, S.V., Jiang, D., Zhang, Y., Dubonos, S.V.: Science **306**(5696), 666–669 (2004)
9. Davis, R.F.: Diamond Films and Coatings. Noyes Publications, Park Ridge (1992)
10. Derjaguin, B.V., Fedoseev, D.V., Lukyanovich, B.V., Spitsyn, A.V., Ryanov, A.F., Lavrentyev, A.V.: J. Cryst. Growth **2**, 380–384 (1968)

11. Prelas, M., Popovicci, G., Bigelow, K. (eds.): Handbook of Industrial Diamonds and Diamond Films. Marcel Dekker, New York (1997)
12. Brand, J., Gadow, R., Killinger, A.: Surf. Coat. Technol. **180**, 213–217 (2004)
13. Bundy, F.B., Hall, H.T., Strong, H.M., Wentorf Jr., R.H.: Nature **176**, 51–55 (1955)
14. Bundy, F.B., Bassettand, W.A., Weathers, M.S., Hemley, R.J., Mao, H.K., Goncharov, A.F.: Carbon **34**, 141–153 (1996)
15. Rossini, F.D., Jessup, R.S.: J. Nat. Bur. Stds. **C21**, 491–497 (1938)
16. Bundy, F.P.: J. Chem. Phys. **38**, 631–643 (1963)
17. Bundy, F.P.: J. Geophys. Res. **85**, 6930–6936 (1980)
18. May, P.W.: Philos. Trans. R. Soc. Lond. A **358**, 473–495 (2000)
19. Simu, U., Karlsson, J., Bjorkman, H., Rangsten, P., Hollman, P.: Limits in Micro Replication of CVD Diamond by Moulding Technique, UPTEC 97 135R (1997)
20. Eversole, W.G.: Synthesis of diamond. U.S. Patents Nos 3030187 and 3030188, 17 April 1962
21. Angus, J.C., Will, H.A., Stanko, W.S.: J. Appl. Phys. **39**, 2915–2922 (1968)
22. Chung, D.D.L.: Materials for Electronic Packaging. Butterworth-Heinemann, Oxford (1995)
23. Haenen, K.: PhD thesis, Limburgs Universitair Centrum, Belgium (2002)
24. Harris, S.J.: Appl. Phys. Lett. **56**, 2298–2300 (1990)
25. Goodwin, D.G., Butler, J.E., Prelas, M.A.: In: Handbook of Industrial Diamonds and Diamond Films. Marcel Dekker, New York (1998)
26. Mankelevich, Y.A., May, P.W.: Diam. Relat. Mater. **17**, 1021–1028 (2008)
27. Bachmann, P.K., Leers, D., Lydtin, H.: Diam. Relat. Mater. **1**, 1–12 (1991)
28. Goss, J.P., Hourahine, B., Jones, R., Heggie, M.I., Briddon, P.R.: J. Phys. Condens. Matter **13**, 8973 (2001)
29. Okaji, M.: Int. J. Thermophys. **916**, 1101–1109 (1998)
30. Wedlake, R.J.: In: Field, J.E. (ed.) The properties of diamond. Academic, London (1979)
31. Jiang, X., Klages, C.P., Zhacai, R., Hartweg, M., Fusser, H.: J. Diam. Relat. Mater. **2**, 407–412 (1993)
32. Iijima, S., Aikawa, Y., Baba, K.: Appl. Phys. Lett. **57**, 2646–2648 (1990)
33. Sawabe, A., Inuzuka, T.: Thin Solid Films **137**, 89–99 (1986)
34. Suzuki, K., Sawabe, A., Yasuda, H., Inuzuka, T.: Appl. Phys. Lett. **50**, 728–729 (1987)
35. Singh, B., Arie, Y., Levine, A.W., Mesker, O.R.: Appl. Phys. Lett. **451**, 526–528 (1988)
36. Chang, C.P., Flamm, D.L., Ibbotson, D.E., Mucha, J.A.: J. Appl. Phys. **63**, 1744 (1988)
37. Kirkpatrick, A.R., Ward, B.W., Economou, N.P.: J. Vac. Sci. Technol. B **7**, 1947–1949 (1989)
38. Denning, P.A., Stevenson, D.A.: Appl. Phys. Lett. **59**, 1562–1564 (1991)
39. Morrish, A.A., Pehrsson, P.E.: Appl. Phys. Lett. **59**, 417–419 (1991)
40. Maeda, H., Ikari, S., Masuda, S., Kusakabe, K., Morooka, S.: Diam. Relat. Mater. **2**, 758–761 (1993)
41. Stoner, B.R., Ma, G.H.M., Wolter, S.D., Glass, J.T.: Phys. Rev. B **45**, 11067–11084 (1992)
42. Jiang, X., Klages, C.P., Zhacai, R., Hartweg, M., Fusser, H.: J. Appl. Phys. Lett. **62**, 3438–3440 (1992)
43. Yang, J., Su, X., Chen, Q., Lin, Z.: Appl. Phys. Lett. **66**, 3284–3286 (1995)
44. Azaroff, L.V., Brophy, J.J.: Electronic processes in materials (1963)
45. Dua, A.K., George, V.C., Friedrich, M., Zahn, D.R.T.: Diam. Relat. Mater. **13**, 74–84 (2004)
46. George, V.C., Das, A., Roy, M., Dua, A.K., Raj, P., Zahn, D.R.T.: Thin Solid Films **419**, 114–117 (2002)
47. George, V.C., Das, A., Roy, M., Dua, A.K., Raj, P., Zahn, D.R.T.: Appl. Surf. Sci. **212–213**, 287–290 (2003)
48. Cui, J.B., Fang, R.C.: J. Phys. D Appl. Phys. **29**, 2759–2762 (1996)
49. Sawabe, A., Inzuka, T.: Appl. Phys. Lett. **46**, 146–147 (1985)
50. Chao, C.H., Popeviei, G., Charison, E.J., Charlson, E.M., Meese, J.M., Prelas, M.A.: J. Cryst. Growth **140**, 454 (1994)
51. Stoner, R.J., Maris, H.J., Anthony, T.R., Banholzer, W.F.: Phys. Rev. Lett. **68**, 1563–1566 (1992)

52. Kromka, A., Janík, J., Balon, F., Kubovic, M., Cerven, I., Dubravcova, V.: Thin Solid Films **433**(1–2), 73–77 (2003)
53. Mahajan, J.R., More, M.A., Patil, P.P., Sainkar, S.R.: Mater. Sci. Eng. **B97**, 117–122 (2003)
54. Shao, Q., Fang, R., Wang, G., Xue, Z.: Prog. Cryst. Growth Charact. Mater. **30**, 221–226 (2000)
55. Dong, L., Zhang, Y., Ma, B., Fu, G.: Diam. Relat. Mater. **11**, 1648–1652 (2002)
56. Johnsson, E., Carlsson, J.O.: Diam. Relat. Mater. **4**, 155–163 (1995)
57. Ashfold, N.R., May, J.P., Petherbridge, W.R., Rosser, K.N., Smith, J.A., Mankelevich, Y.A., Suetin, N.V.: Phys. Chem. Chem. Phys. **3**, 3471–3485 (2001)
58. Hirakuri, K.K., Kobayashi, T., Nakamura, E., Mutsukura, N., Friedbacher, G., Machi, Y.: Vacuum **63**, 449–454 (2001)
59. Knotek, O., Bosch, W., Leyendecker, T., Munz, W.D., Falkenstein, R.: 8th ICVM, Linz, vol. C11.2, p. 340 (1985)
60. Rudder, R.A., Hudson, G.C., Posthill, J.B., Thomas, R.E., Hendry, R.C., Malta, D.P., Markunas, R.J., Humphreys, T.P., Nemanich, R.J.: Appl. Phys. Lett. **60**, 329–331 (1992)
61. Bozeman, S.P., Tucker, D.A., Stoner, B.R., Glass, J.T., Hooke, W.M.: Appl. Phys. Lett. **66**, 3579–3581 (1995)
62. Noda, H., Nagai, H., Shimakura, M., Hiramatsu, M., Nawata, M.: J. Vac. Sci. Technol. A **16** (6), 3170–3174 (1998)
63. Ng, K.K., Liew, Y.S., Md Nor, R., Wong, C.S.: Jurnal Fizik Malaysia **23**(1–4), 51 (2001)
64. Liew, Y.S.: MSc thesis, University of Malaya (2002)
65. Tan, C.H., Ng, K.H., Md Nor, R., Wong, C.S.: Jurnal Fizik Malaysia **25**(3–4) (2004)
66. Menon, P.M., Edwards, A., Feigerle, C.S., Shaw, R.W., Coffey, D.W., Heatherly, L., Clausing, R.E., Robinson, L., Glasgow, D.C.: Diam. Relat. Mater. **8**, 101–109 (1999)
67. Vogel, T., Meijer, J., Zaitsev, A.: Diam. Relat. Mater. **13**, 1822–1825 (2004)
68. Li, R., Hu, X., Shen, H., He, X.: Mater. Lett. **58**, 1835–1838 (2004)
69. Borst, T.H., Weis, O.: Diam. Relat. Mater. **4**, 948–953 (1995)
70. Suzuki, M., Yoshida, H., Sakuma, N., Ono, T., Sakai, T., Ogura, M., Okushi, H., Koizumi, S.: Diam. Relat. Mater. **13**, 198–202 (2004)
71. Latto, M.N., Roley, D.J., May, P.W.: Diam. Relat. Mater. **9**, 1181–1183 (2000)
72. Bohr, S., Haubner, R., Lux, B.: Diam. Relat. Mater. **4**, 133–144 (1995)
73. Koizumi, M., Kamo, Y., Sato, S., Mita, A., Sawabe, A.: Diam. Relat. Mater. **7**, 540–544 (1998)
74. Tsang, R.S., May, P.W., Ashfold, M.N.R., Rosser, K.N.: Diam. Relat. Mater. **7**, 1651–1656 (1998)
75. Petherbridge, J.R., May, P.W., Fuge, G.M., Rosser, K.N., Ashfold, M.N.R.: Diam. Relat. Mater. **11**, 301–306 (2002)
76. Petherbridge, J.R., May, P.W., Fuge, G.M., Robertson, G.F., Rosser, K.N., Ashfold MNR, J.: Appl. Phys. **91**(6), 3605–3615 (2002)
77. Mikka, N.G., Yasu, E., Xiao, C., Kikuchi, Y., Yushiwaza, K., Sakaguchi, T., Suzuki, T., Ando, T.: Diam. Relat. Mater. **9**, 941–947 (2000)
78. Harshavardhan, K.S., Vijayarahavan, M.N., Chandrabhas, N., Sood, A.K.: J. Appl. Phys **68**(7), 3303–3306 (1990)
79. Vittone, E., Manfredotti, C., Fizzotti, F., Lo Giudice, A., Polesello, P., Ralchenko, V.: Diam. Relat. Mater. **8**, 1234–1239 (1999)
80. Vinokur, N., Miller, B., Avyigal, Y., Kalish, R.: J. Electrochem. Soc. **143**, L238 (1996)
81. Zhu, W., Kochanski, G.P., Lin, S., Seibles, L.: J. Appl. Phys. **78**, 2707–2711 (1995)
82. May, P.W.: Science **319**, 1490–1491 (2008)